Case Studies in Construction Materials 5 (2016) 87–99

Contents lists available at ScienceDirect

Case Studies in Construction Materials

journal homepage: www.elsevier.com/locate/cscm

Case study

Indoor accelerated corrosion test and marine field test of corrosion-resistant low-alloy steel rebars

Ming Liu[a], Xuequn Cheng[a], Xiaogang Li[a,b,*], Jiezhen Hu[c], Yue Pan[a], Zhu Jin[a]

[a] Corrosion and Protection Center, University of Science and Technology Beijing, Beijing 100083, China
[b] Ningbo Institute of Material Technology & Engineering, Chinese Academy of Sciences, Ningbo 315201, Zhejiang, China
[c] Engineering College,Guangdong Ocean University, Zhanjiang 524088, China

ARTICLE INFO

Article history:
Received 17 June 2016
Received in revised form 20 August 2016
Accepted 12 September 2016
Available online 4 October 2016

Keywords:
Chromium
Rebar
Macrocell corrosion test
Corrosion products
Corrosion rate
Marine field test

ABSTRACT

Macrocell corrosion test and accelerated alternating wet–dry experiment combined with marine field test were employed to study the corrosion behavior of HRB400 carbon steel, 1.5Cr steel, and 5Cr steel in a simulated concrete pore solution and mortar. The macrocell current significantly decreases in samples added with Cr compared with that in HRB400 steel. The corrosion rate is decreased by Cr but increased by Cl^-; as a consequence, the corrosion rates of 1.5Cr and 5Cr steel are lower than that of HRB400 steel. However, the corrosion products differ slightly in terms of the contents of α-FeOOH (goethite), γ-FeOOH (lepidocrocite), γ-Fe_2O_3, and Fe_3O_4 (maghemite or magnetite). The addition of Cr increases the content of the protective α-FeOOH and reduces the content of γ-FeOOH. Both ordinary and high-performance epoxy coatings remain intact after 1 year of marine field test. Among the bare steel rebars, HRB400 steel shows extensive localized corrosion on the surface, whereas 1.5Cr steel exhibits less severe corrosion. The scarcely visible corroded areas in 5Cr steel indicate that this rebar is in the passive state, consistent with results of the indoor accelerated test. Hence, the durability of concrete structures can be prolonged with the utilization of corrosion-resistant low-alloy rebars.
© 2016 The Authors. Published by Elsevier Ltd. This is an open access article under the CC BY-NC-ND license (http://creativecommons.org/licenses/by-nc-nd/4.0/).

1. Introduction

Accidents caused by failure of concrete constructions ahead of time commonly occur because of corrosion of rebars, which are widely used in concrete constructions, leading to significant economic loss [1–3]. Corrosion-resistant rebars are rarely utilized, although stainless steel rebars exhibit excellent corrosion resistance in harsh corrosive media [4–6]. For the high cost of stainless steel, which is six to seven times higher than that of carbon steel, restricts its use in engineering constructions. To enhance the corrosion resistance of rebars, Gareth [7] developed an MMFX steel rebar with low carbon content and 9%–11% Cr. Gong et al. [8] fabricated MMFX rebars with excellent corrosion resistance in simulated concrete pore solution; the corrosion rate of the rebar is 1/3–1/2 higher than that of carbon steel. Corrosion-resistant low-alloy rebars have become a research hotspot; these rebars can be developed using the optimum design based on plain carbon steel. Nevertheless, research on corrosion-resistant rebars remains in its early stages. Singh et al. [9] reported that addition of small amounts of Cu and Cr to carbon steel can decrease the corrosion rate in simulated concrete pore solution. Guo et al. [10]

* Corresponding author at: Corrosion and Protection Center, University of Science and Technology Beijing, Beijing 100083, China.
E-mail address: lixiaogang@ustb.edu.cn (X. Li).

http://dx.doi.org/10.1016/j.cscm.2016.09.005
2214-5095/© 2016 The Authors. Published by Elsevier Ltd. This is an open access article under the CC BY-NC-ND license (http://creativecommons.org/licenses/by-nc-nd/4.0/).

performed salt spray tests and dry-wet cyclic immersion and concluded that adding Nb and Re enhances the corrosion resistance of rebars. Ai et al. [11] investigated the passivation behavior of Cr8Ni2 alloy corrosion-resistant rebar in simulated concrete pore solutions with different pH values (13.5–9.0) and found that Cr8Ni2 steel can maintain a stable passive state at low pH values.

Field experiments for evaluation of the durability of rebars require a long time and huge amount of effort because of the specificity of rebar corrosion in concrete. Therefore, indoor accelerated corrosion tests have been developed to shorten the experimental cycle, and the results can reflect the corrosion degrees of rebars, corrosion rates, and threshold concentrations of chloride; these tests can be used to assess the corrosion resistance of rebars and estimate service life in a relatively short experimental cycle (less than 2 years). Corrosion-resistant properties can be evaluated with macrocell corrosion test [12], potentiodynamic scanning test [13], potentiostatic polarization test [14], dry–wet cycle test [15], and ASTM G109 test [16].

In our previous work, Cr-modified corrosion-resistant low-alloy rebars exhibit high threshold concentration of chloride and low corrosion rate in saturated calcium hydroxide solution [17]. However, simulated concrete pore solution may differ from practical service conditions in concrete because of porosity; in addition, surface condition of rebars considerably affect the corrosion behavior [18–20]. In this paper, macrocell corrosion test, alternating dry–wet corrosion test, and 1-year marine field study were conducted in the splash zone in Zhanjiang seawater corrosion station to study the corrosion behavior of corrosion-resistant low-alloy reinforced samples. Results provide insights into research and development of corrosion-resistant low-alloy rebars.

2. Experimental procedures

2.1. Materials

In this work, HRB400 carbon steel rebar and two Cr-modified low alloy steel rebars were used for experiments [17]. Table 1 shows the chemical composition (in% by mass) of the three kind of steel rebars determined by analytical analysis. The diameter of HRB400 steel and 1.5Cr steel is 16 mm, and that of 5Cr steel is 22 mm.

2.2. Macrocell corrosion test

The test method is based on ASTM 955/955M-09a [12]. Three types of rebars (125 mm in length) were used. Prior to testing, burrs on the end region were removed; one end was drilled a threaded hole, which was passed through with a 10 mm-long stainless screw connected to a copper wire with 1.5 mm^2 cross-sectional area; the joint was sealed with epoxy coating to prevent crevice corrosion; the specimens were degreased and cleaned for use. The cathode consisted of two rebars and simulated concrete pore solution; 1L of the solution contained 18.81 g KOH, 974.8 g distilled water, and 17.87 g NaOH. The anode consisted of a rebar and simulated concrete pore solution containing 15 wt.% NaCl. The solution was prepared and replaced every 5 weeks by mixing deionized water and analytical grade reagent. Tests were performed at room temperature was approximately 25 °C for 15 weeks.

Fig. 1 shows the simulated concrete pore solution containing NaCl adjacent to the anode (75 mm high); the rebar was placed at the center bottom, and its top passed through the plastic cover above the liquid level. The copper wire at the end of rebar was connected to the black terminal. Near the cathode, the height of the liquid in the simulated concrete pore solution was 75 mm. Two rebars were placed and fixed with a plastic cover on top of the chamber. Copper wires at the end of the rebars were linked with another wire connected to the red terminal. Prior to testing, the cathodic chamber was purged with scrubbed air to drain CO_2 in solution. The cathode and the anode were jointed by a salt bridge. The salt bridge was made up of KNO_3 and agar, which was intended to reduce the pollution of chlorine ion.

A multimeter was connected to the two terminals of a 10 Ω resistor to measure voltage drop. The negative pole of the resistor was connected to the black terminal, and the positive pole was linked to the red terminal. After measuring the voltage drop, the anode was removed from the terminal box for 2 h. A saturated calomel electrode (SCE) was used as reference electrode to measure anodic and cathodic potential. Readings on the multimeter were recorded every day in the first week and once a week thereafter.

The voltage drop was converted to corrosion rate (μm/a) with the following formula:

$$\text{Corrosion rate} = 11.6 \cdot i_c = 11600 \cdot V/(A \cdot R) \quad (1)$$

Table 1
Chemical composition (wt.%) of the tested steel rebars.

Steel	C	Si	Mn	P	S	Cr	Fe
HRB400	0.196	0.57	1.57	0.024	0.017	0.08	residual
1.5Cr	0.171	0.66	1.30	0.014	0.008	1.50	residual
5Cr	0.157	0.45	1.57	0.010	0.004	5.06	residual

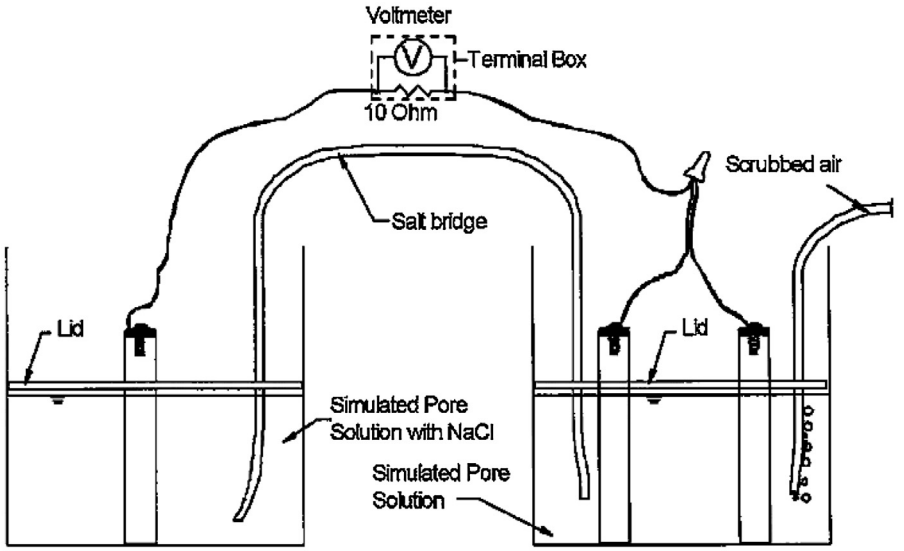

Fig. 1. Schematic of the experimental set-up for macrocell corrosion test [12].

where i_c is the corrosion current density ($\mu A/cm^2$); V is the voltage drop observed in the 10 Ω resistor (mV); R is the resistance (Ω); and S is the area of the bare rebar of the cathode (cm^2).

2.3. Alternating wet–dry experiment

The experimental solution was saturated $Ca(OH)_2$ (CH) solution [17,21] containing 0%, 0.05%, 0.1%, 0.25%, 0.5%, and 1.0% NaCl. The temperature of the solution was approximately 25 °C, and the maximum temperature of the drying chamber was 35 °C for each test cycle which lasted for 60 min, wherein the immersing time was 12 min; the etching time was 144 h.

Specimens were as-received steel rebars with a length of 50 mm; three parallel samples were adopted in each test; prior to test, all specimens were cleaned with deionized water and ethyl alcohol, blow-dried, and finally weighed; and the initial weight was marked as w_0 (the accuracy was 0.001 g). Corrosion rate was calculated with the following formula:

$$v = \frac{8.76 \times 10^4 \times W}{S \times t \times \rho} \tag{2}$$

where v stands for the corrosion rate (mm/a); W is the weight loss (g); S is the surface area of a specimen (cm^2); ρ represents the density of the metal (g/cm^3); and t is the test cycle (h).

The corrosion products were removed by ultrasonic cleaning in descaling liquid (500 ml HCl + 500 ml H_2O + 3–10 g Aci-Steril) for 3 min, followed by ultrasonic cleaning in deionized water, and then cleaned with acetone and blow-dried. The corrosion products were analyzed with D/max-rA transfer target polycrystal X-ray diffractometer. In this work, UltimalV X-ray diffractometer was used with copper target; the tube voltage and tube current were 40 kV and 40 MA, respectively; the scanning range was 10°–90° and the scanning rate was set at 4°/min. The corrosion products were scraped off mechanically and ground into powder with particles that are less than 10 μm to acquire a fine grain size without any preferred orientation. Before XRD tests, the glass plate was filled with the powder-like corrosion products and acetone was dropped in for fixation.

2.4. Marine field test

The specimens used were bare corrosion-resistant rebars and rebars with epoxy coatings, including ordinary epoxy coatings (fabricated according to the Chinese National Standard GB/T25826-2010 [22] and Chinese Construction Industry Standard JG3042-1997 [23]) and high-performance epoxy coatings (fabricated according to technical regulations made by Chinese Academy of Science [24]). Ordinary epoxy coated steel rebars and high performance epoxy coated steel rebars are processed by the Institute of Metal Research, Chinese Academy of Sciences.

The dimensions of the specimens were 40 mm × 40 mm × 200 mm. The diameter of HRB400 and 1.5Cr steel was 16 mm, whereas the diameter of the 5Cr steel was 22 mm. The protective layer was 9–12 mm thick. Ordinary Portland cement, P.O 42.5, drinking water, river sand, fineness modulus of 2.7 were chosen, and the pouring proportion of the mortar for cement: water: sand = 1:0.5:2.5 with dimensions of 40 mm × 40 mm × 200 mm; and the diffusion coefficient was 1.56 cm^2/a. The length of the rebar was 250 mm, of which 25 mm of both ends were exposed, as shown in Fig. 2. Prior to testing, the rebars were pickled with 12 wt.% HCl solution, rinsed, neutralized with whitewash, washed with water, wiped dry, and then placed

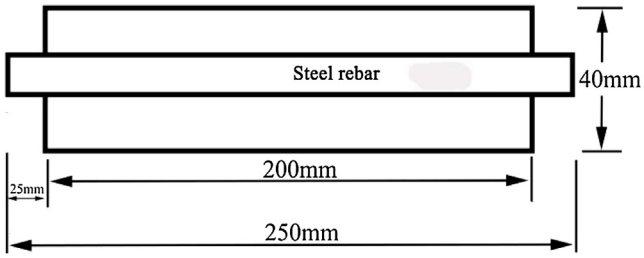

Fig. 2. Schematic of concrete samples for the marine field study.

in a dryer for 4 h. Before the molding of samples, the rebars covered with batter board were placed in the mold, and the batter board was attached close to the two end plates of the mold; after proper placement, the surfaces of the rebars were cleaned with acetone. After molding, the samples were conserved by covering them with a wet cloth for 24 h at $(20 \pm 2)\,^{\circ}C$, followed by numbering and removal of the batter board. The samples were then placed in standard curing room for 28 d. The field study was carried out in the seawater corrosion test station in the splash zone at Naozhou island in Zhanjiang, Guangdong Province in China for 1 year (Fig. 3), and three parallel samples were used in every group.

3. Results and discussion

3.1. Macrocell corrosion test

Fig. 4 shows the variation of cathodic and anodic potential (vs. SCE) with time. Based on Fig. 4(a), the anodic potential of HRB400 steel fluctuates within −470–550 mV, and tends to stabilize at a value more negative than −530 mV as time elapses; the cathodic potential of HRB400 steel fluctuates within the range of −190–250 mV; observations show that when a rebar is in a passive state, the open circuit potential is more positive than −276 mV (vs. SCE) [25]; therefore, we deduce that the cathode of HRB400 steel is in passivation. As shown in Fig. 4(b), in the initial period, the anodic potential of 1.5Cr steel fluctuates within the range of −480–550 mV and tends to stabilize at a value a little more negative than −500 mV; the cathodic potential is about −200–240 mV; therefore, the cathode of 1.5Cr steel is in a passive state. In Fig. 4(c), the anodic potential of 5Cr steel varies within −480–540 mV with a slight fluctuation; as time passes by, the anodic potential gradually stabilizes around −510 mV; the cathodic potential is about −180–230 mV, which indicates that the cathode is in passivation.

Fig. 5 shows the variation in the corrosion rate of rebars with time. In the initial period, the corrosion rates of the three parallel samples are consistent; corrosion rate declines and then stabilizes as time elapses, confirming the results for the anodic potential. The average corrosion rate of the three types of steel is shown in Fig. 6, which illustrates that the corrosion rate of HRB400 steel is the highest; 1.5Cr steel has the second highest corrosion rate (71% of corrosion rate of HRB400 steel, and corrosion resistance is enhanced by 1.4 times) and that of 5Cr is the lowest (40% corrosion rate of HRB400 steel, and corrosion resistance increases by 2.5 times). The results demonstrate that the addition of Cr improves the corrosion resistance of rebars in simulated concrete pore solution. The corrosion morphology of anodic rebars after the experiment is shown in Fig. 7. Numerous corrosion products exist on the surface of anodic rebars; apparently, the corrosion degree of HRB400 steel is more severe, coinciding with the results on the corrosion rate.

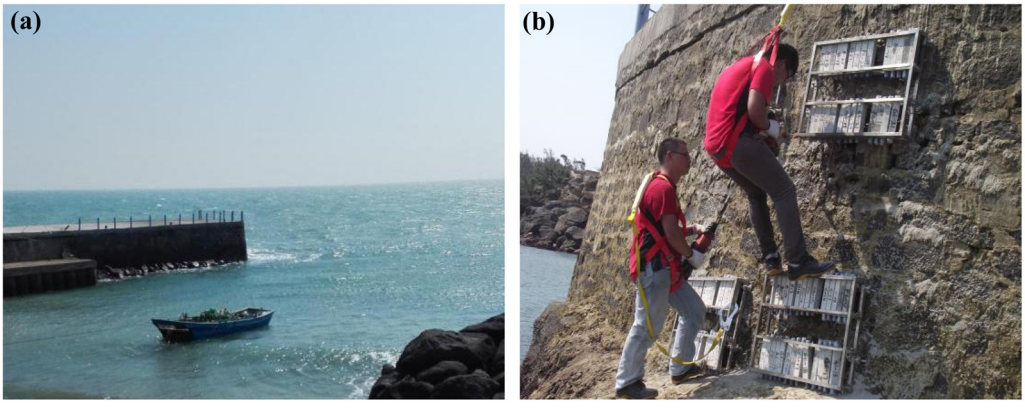

Fig. 3. Construction photograph of marine field concrete samples in Zhanjiang, Guangdong, China. (a) Naozhou island in Zhanjiang, (b) field construction after falling tide.

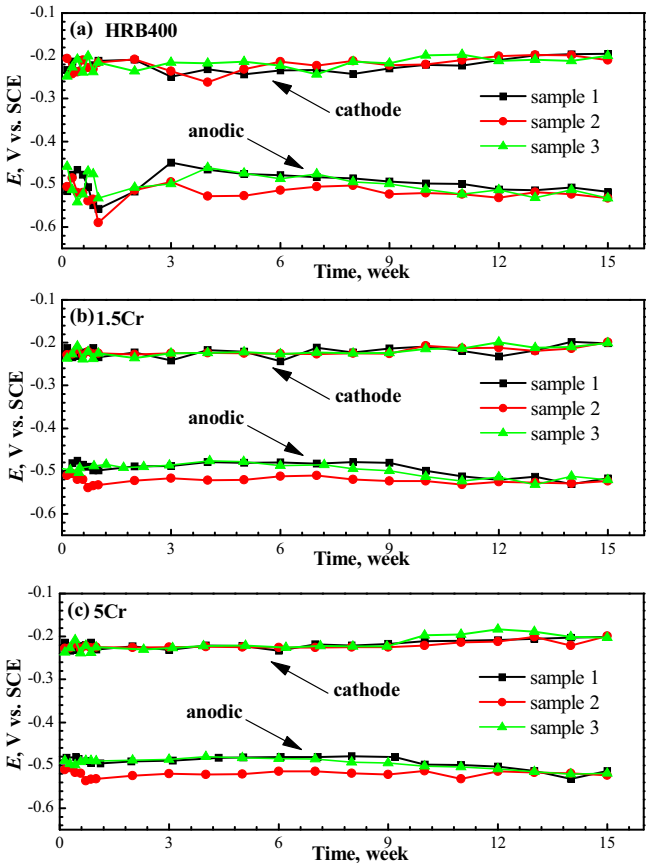

Fig. 4. The macrocell corrosion potential of rebars.

3.2. Alternating dry-wet experiment

Fig. 8 shows the corrosion morphology of rebars after an 8-day alternating dry-wet test in a simulated concrete pore solution with various Cl^- concentration. As shown in Fig. 8, localized corrosion is dominant; as the concentration of Cl^- increases, corrosion products increase and corrosion is intensified; in addition, in the simulated concrete pore solution with a specific Cl^- concentration, the corrosion degree are sorted from serious to mild as follows: HRB400 > 1.5Cr > 5Cr.

Fig. 9 shows the relationship between the corrosion rate of steel rebar and Cl^- concentration in CH solution after the 8-day alternating dry-wet test. As shown in Fig. 9, adding Cl^- aggravates corrosion. When Cl^- concentration increases from 0 to 0.5 wt.%, the corrosion rate rapidly increases, whereas corrosion rate rises in small increments after Cl^- concentration reaches 0.5 wt.%. In CH solution with a specific Cl^- concentration, the corrosion rate of HRB400 steel is the highest; 1.5Cr steel is the second highest; and 5Cr steel has the lowest corrosion rate, which is half of that of HRB400 steel. Thus, the addition of Cr obviously improves corrosion resistance, which is consistent with results of the macrocell corrosion test.

The corrosion products of steel rebars in CH solution containing 1 wt.% NaCl used in the 8-day alternating dry-wet test were analyzed with X-ray diffraction (XRD). The results are shown in Fig. 10. The corrosion products of the three types of steel have the same chemical composition: α-FeOOH (Goethite), γ-FeOOH (Lepidocrocite), and γ-Fe_2O_3/Fe_3O_4. However, as the Cr content increases, the diffraction peak of α-FeOOH rises whereas that of γ-FeOOH decreases, indicating that adding Cr increases the content of α-FeOOH and reduces γ-FeOOH in the corrosion products. For verification purposes, semi-quantitative analysis of corrosion products is adopted through RIR values (form PDF cards) by using HighScore Software.

As shown in Fig. 10, the content of α-FeOOH is sorted from highest to lowest as follows: 5Cr > 1.5Cr > HRB400; the content of γ-FeOOH from highest to lowest is: HRB400 > 1.5Cr > 5Cr. γ-FeOOH is an intermediate product of the electrochemical corrosion process of rebars, and it usually acts as reductor to accelerate corrosion resulting from strong electrochemical activity; by contrast, α-FeOOH is the most abundant iron oxide hydroxide, and the major component in the protective rust layer due to the insulation and weak electrochemical activity. Subsequently, the ratio of α-FeOOH content to γ-FeOOH content ("α/γ") is used to characterize the protective capability of rust layer in rebars: i.e., a higher "α/γ" means that the corrosion products are more stable and they can prevent the matrix from being corroded [26–29]. As shown in Fig. 11, the "α/γ" values of HRB400, 1.5Cr, and 5Cr steel are 0.242, 0.375, and 0.687, respectively, which indicates that the corrosion

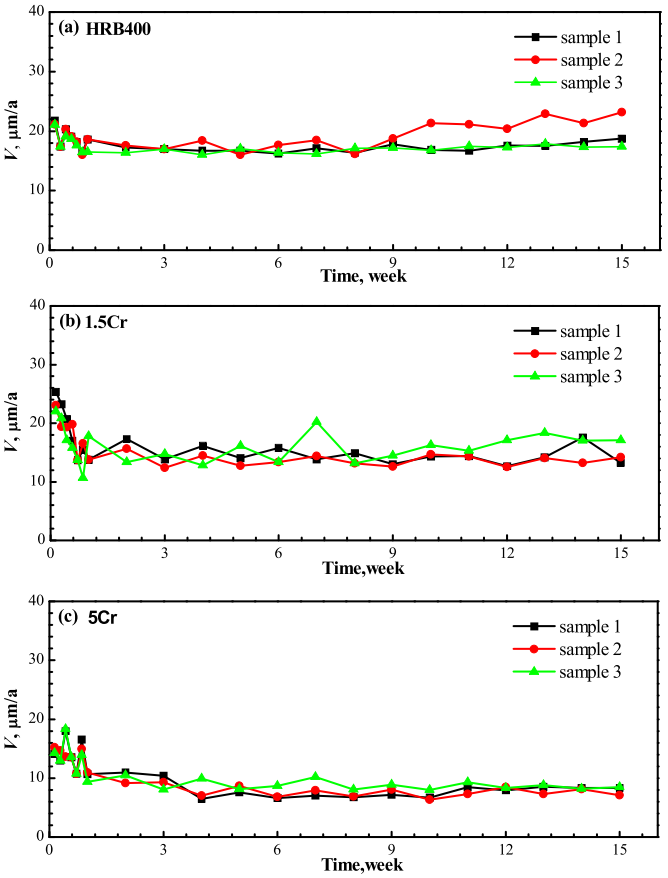

Fig. 5. Macrocell corrosion rate of rebars.

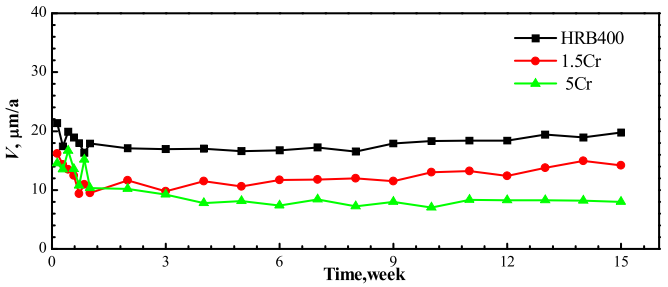

Fig. 5. Macrocell corrosion rate of rebars.

products of 5Cr are the most protective; those of 1.5Cr are the second most protective, and those of HRB400 are the least protective; thus, the order of the corrosion resistance of the three types of rebars from good to bad is: 5Cr > 1.5Cr > HRB400.

3.3. Analysis of marine field studies

The two-stage service life model first proposed by Tuutti in 1982 [30]. The first stage is the corrosion induced by chloride ions. The initiation period t_i is the time needed for sufficient chlorides to penetrate the cover and accumulate in sufficient quantity up to the depth of the embedded steel and ultimately initiate corrosion of the steel. The most commonly used chloride ion diffusion equations are mostly based on Fick's second law [30–32]:

$$C_x = (C_s - C_0)\left[1 - erf\left(\frac{x}{2\sqrt{Dt}}\right)\right] + C_0 \tag{3}$$

where

C_x is the chloride ion concentration of a concrete surface at x,

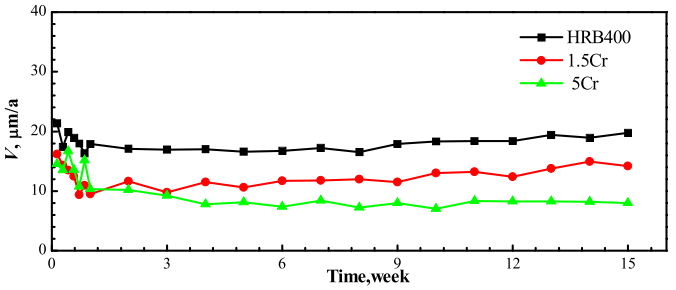

Fig. 6. Average corrosion rate of rebars.

Fig. 7. Corrosion morphology of anodic rebars after a 15-week macrocell corrosion test.

C_s is the constant chloride concentration at the surface of concrete,
C_0 is the constant initial chloride concentration of concrete,
D is the constant chloride ion diffusion coefficient of concrete,
x is the depth from the exposed surface,
erf(g) is the E_{rror} function, and
t is the time since exposure to surface chloride.

The propagation period t_p is the time necessary for sufficient corrosion to occur to cause an unacceptable level of damage to the structure or structural member under consideration. The length of this period depends not only on the rate of the corrosion but also on the definition of "unacceptable damage". This level of damage varies depending on the requirements of the owner and the nature of the structure.

To accelerate the corrosion of rebars, the thickness of the protective layer was reduced to speed up the diffusion of Cl^-. According to our previous work, the chloride threshold levels of HRB400, 1.5Cr and 5Cr steel rebars in CH solution are: 1.2 wt.%, 2.8 wt.% and 7.4 wt.% NaCl, respectively [17].

According to Yamaji [32], the content of chloride ion in CH solution can be transformed into the content of chloride ion in concrete. The specific calculation process is as follows:

(1) Quantity of pore solution

The amount per unit volume of pore solution in concrete can be calculated with water (kg/m^3), cement (kg/m^3), and the ratio of water and cement h (%):

$$p = \frac{W - c \times h}{1000} \times 100\% \tag{4}$$

where $h = 20\%$, $W = 150\,kg/m^3$, $C = 300\,kg/m^3$ ($W/C = 0.5$), and $p = 9.0\%$.

(2) Free chloride ion concentration in concrete

The free chloride ion, C_v (kg/m^3), in concrete can be calculated with P and the concentration of Cl^- in CH solution, a (%):

$$C_v = 1000 \times \frac{a}{1 - a} \times p \tag{5}$$

(3) Fixed chloride ion concentration in concrete

The fixed chloride ion concentration of cement, a_{fix} (%), is calculated by the following formula:

$a_{mob} < 0.358$, $a_{fix} = 4.74 \times a_{mob}$ (6)

$a_{mob} \geq 0.358$, $a_{fix} = 0.240 \times a_{mob} + 1.615$

Fig. 8. Corrosion morphology of steel bar in CH solution with different Cl^- concentrations during an 8-day alternating dry-wet test (In each picture, the steel bars are 1.5Cr, 5Cr and HRB400 from the left to the right.).

where a_{mob} is the percentage of cement quality ratio and can be calculated from the chloride ion concentration in the simulated concrete solution:

$$a_{mob} = a \times \frac{W}{C} \tag{7}$$

(4) Fixed chloride ion concentration in concrete

The fixed chloride ion in concrete C_{fix} (kg/m^3) using calculated using a_{fix} and cement content:

$$C_{fix} = C \times \frac{a_{fix}}{100} \tag{8}$$

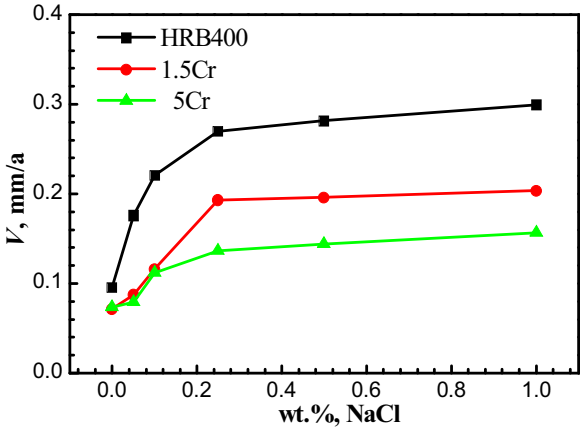

Fig. 9. Relationship of corrosion rate of steel rebars and Cl^- concentration in CH solution during 8-day alternating dry–wet test.

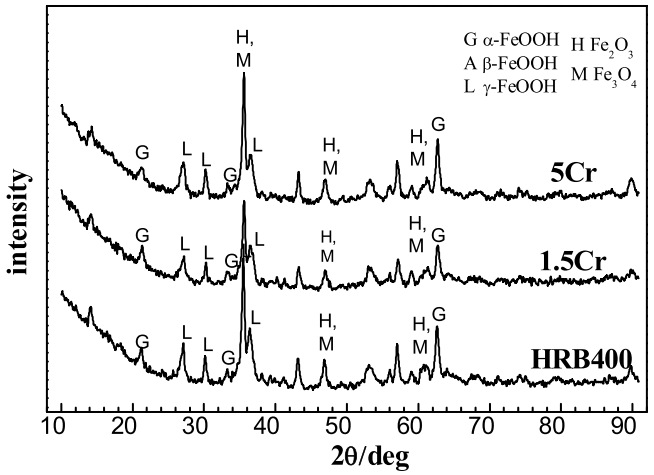

Fig. 10. XRD diagram of rebars after the 8-day alternating dry-wet test in CH solution with 1% NaCl.

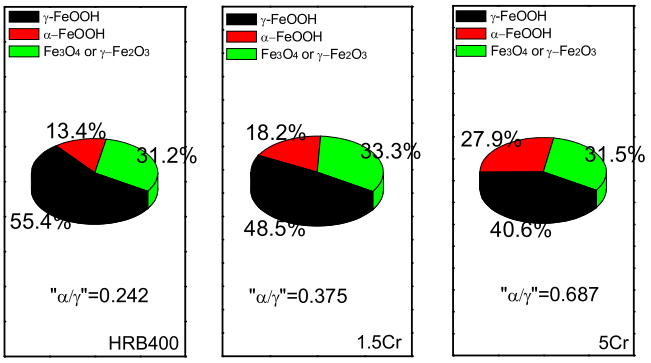

Fig. 11. Semi-quantitative analysis of corrosion products of rebars after the 8-day alternating dry-wet test in CH solution with 1% NaCl.

(5) Total chloride ion concentration

The total chloride ion concentration in concrete can be expressed as follows:

$$C_{tot} = C_v + C_{fix}C_{tot} \tag{9}$$

From the experimental results, the CTL of the steel rebars in CH solution are converted to total chloride ion in concrete, as shown in Table 2.

The time when steel starts to corrode in concrete is calculated with the following equation [32]:

$$C_d = \gamma_{cl}C_0\left[1 - erf\left(\frac{0.1c}{\sqrt[2]{D_d t_i}}\right)\right] \tag{10}$$

where C_d is the CTL; γ_{cl} is the fluctuation coefficient, which is generally equal to 1; and C_0 is the surface chloride concentration, considering that the marine splash zone is the most severely corrosive area, and the surface chloride concentration can reach a maximum value in a very short period of time with a value of 15.1 kg/m^3. C is the thickness of the concrete protective layer. D_d is the chloride ion diffusion coefficient, 1.56 cm^2/a [30]. Table 3 lists the calculation parameter values.

From Table 3, the initiation corrosion time of rebars during the 1-year field test in the splash zone in Zhanjiang is predicted, as shown in Table 4; the initiation corrosion time of HRB400 steel is 0.47 year, and those of 1.5Cr steel and 3Cr steel are 0.63 and 1.15 years, respectively. Based on the predicted values, HRB400 and 1.5Cr steel rebars are in rust developing stage whereas 5Cr steel rebar is still in the passive state after the 1-year test.

Fig. 12 shows the macromorphology of the three kinds of bare rebars covered with ordinary epoxy coatings and another set covered with high-performance epoxy coatings after the 1-year field test in the splash zone in Zhanjiang. The mortar is integrated without any obvious cracks.

Fig. 13 shows the corrosion morphology of the three kinds of bare rebars after the removal of the concrete layer. Apparently, localized corrosion occurs in the HRB400 steel and 1.5Cr steel, and the corrosion of 1.5Cr steel is relatively mild. No corroded region is visible on the surface of 5Cr steel; in other words, 5Cr steel is in a passive state, which confirms the predicted results in Table 3. In conclusion, 5Cr steel exhibits the highest chloride threshold concentration level and excellent corrosion resistance.

The corrosion products of HRB400 steel and 1.5Cr after the 1-year field test in the splash zone in Zhanjiang were analyzed with X-ray diffraction (XRD), and the results are shown in Fig. 14. The corrosion products of the two steel rebar samples have

Table 2
The calculated chloride ion in concrete.

Steel	NaCl (wt.%)	C_v (kg/m^3)	C_{fix} (kg/m^3)	C_{tot} (kg/m^3)
HRB400	1.2	0.66	5.11	5.77
1.5Cr	2.8	1.56	5.45	7.01
5Cr	7.4	4.23	6.46	10.69

Table 3
Calculation parameters of concrete life prediction.

parameters		
	cement *W*/*C*	0.50
	D_d(cm^2/a)	1.56
	C_0(kg/m^3)	15.1(marine splash zone)
	c(mm)	12 (HRB400, 1.5Cr), 9 (5Cr)

Table 4
Initiation corrosion time of steel embedded in reinforced concrete (marine splash zone).

Steel	*d* mm	*c* mm	CTL kg/m^3	t_i year
HRB400	16	12	5.77	0.47
1.5Cr	16	12	7.01	0.63
5Cr	22	9	10.7	1.15

Fig. 12. Macromorphology of rebars after a 1-year field test in the splash zone in Zhanjiang.

Fig. 13. Corrosion morphology of three kinds of bare rebars after a 1-year field test in the splash zone in Zhanjiang.

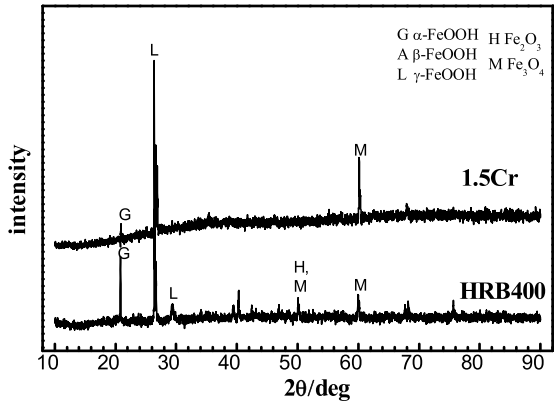

Fig. 14. XRD pattern of HRB400 and 1.5Cr rebars after the 1-year field test in the splash zone in Zhanjiang.

Fig. 15. Corrosion morphology of the three kinds of rebars covered with ordinary epoxy coatings after the removal of concrete layer.

Fig. 16. Corrosion morphology of the three kinds of rebars covered with high-performance epoxy coatings after the removal of the concrete layer.

the same chemical composition: α-FeOOH (Goethite), γ-FeOOH (Lepidocrocite), and γ-Fe_2O_3/Fe_3O_4. The corrosion products are the same for the accelerated alternating wet–dry test. The experimental results show that accelerated alternating wet–dry corrosion test has high relevance and consistency with the 1-year field test in the splash zone. accelerated alternating wet–dry corrosion test can then be used as a quick way to evaluate the corrosion resistance of steel rebars.

Figs. 15 and 16 show the corrosion morphology of the three kinds of rebars covered with ordinary epoxy coatings and with high-performance epoxy coatings after the removal of concrete layer, respectively. The coatings are intact without any visible rust spots, which indicate that the application of epoxy coatings can improve the corrosion resistance of rebars.

4. Conclusion

Through indoor accelerated corrosion test and marine field studies of HRB400 steel, 1.5Cr steel, and 5Cr steel, the conclusions we draw are summarized as follows:

(1) HRB400 steel exhibits poor corrosion resistance; as the Cr content is increased, the corrosion rate is reduced; corrosion rate of 5Cr steel is the lowest and merely half that of the corrosion rate of HRB400.
(2) The primary corrosion products of steels are α-FeOOH, γ-FeOOH, and γ-Fe_2O_3/Fe_3O_4; in 1.5Cr steel and 5Cr steel, protective α-FeOOH is the most dominant among the corrosion products, indicating that Cr promotes the formation of protective corrosion products.
(3) After a 1-year field study in the splash zone in Zhanjiang, ordinary epoxy coatings and high-performance epoxy coatings are still intact without any obvious corroded zones; among the bare rebars, HRB400 and 1.5Cr steel present localized corrosion, whereas 5Cr steel does not have any corroded zone on its surface. Results of field study coincide with the predicted results, which prove that the utilization of corrosion resistant rebars can improve the durability of concrete structures.

Acknowledgments

This work was supported by the National Science and Technology Infrastructure Platforms Construction Project and the National Basic Research Program of China (973 Program project, No.2014CB643300).

References

[1] Y.S. Choi, S.T. Yi, M.Y. Kim, et al., Effect of corrosion method of the reinforcing bar on bond characteristics in reinforced concrete specimens, Constr. Build. Mater. 54 (3) (2014) 180–189.
[2] S. Patil, B. Karkare, S. Goyal, et al., Acoustic emission vis-à-vis electrochemical techniques for corrosion monitoring of reinforced concrete element, Constr. Build. Mater. 68 (2014) 326–332.
[3] V. Mahdi, S. Mohammad, G. Pouria, Comparative studies of experimental and numerical techniques in measurement of corrosion rate and time-to-corrosion-initiation of rebar in concrete in marine environments, Cem. Concr. Compos. 48 (2014) 98–107.
[4] J.J. Shi, W. Sun, Recent research on steel corrosion in concrete, J. Chin. Ceram. Soc. 38 (9) (2010) 1753–1764.
[5] M. Criado, D.M. Bastidas, S. Fajardo, A. Fernández-Jiménez, J.M. Bastidas, Corrosion behaviour of a new low-nickel stainless steel embedded in activated fly ash mortars, Cem. Concr. Compos. 33 (6) (2011) 644–652.
[6] L. Freire, M.J. Carmezima, M.G.S. Ferreira, et al., The electrochemical behaviour of stainless steel AISI 304 in alkaline solutions with different pH in the presence of chlorides, Electrochim. Acta 56 (2011) 5280–5289.
[7] Ricardo R. De Rojas, New Developments in Steel Protection from Corrosion, Massachusetts institute of technology, 2001.
[8] L. Gong, D. Darwin, J.P. Browning, et al., Evaluation of mechanical and corrosion properties of MMFX reinforcing steel for concrete, A Report on Research Sponsored, Kansas Department of Transportation, Topeka, Kansas, 2004, pp. 1131 (FHWA-KS-02-8).
[9] J.K. Singh, D.D.N. Singh, The nature of rusts and corrosion characteristics of low alloy and plain carbon steels in three kinds of concrete pore solution with salinity and different pH, Corros. Sci. 56 (2012) 129.
[10] Z. Guo, W.G. Wan, W. Sun, et al., Study on high strength and resisting corrosion steel bar containing Re, Iron Steel 45 (12) (2012) 53–58.
[11] Z.Y. Ai, J.J. Jiang, W. Sun, et al., Passive behaviour of Cr8Ni2 alloy corrosion-resistant steel in simulating concrete pore solutions with different pH values, J. Southeast Univ. (Natr. Sci. Ed.) 1 (2016) 152–159.
[12] D. Darwin, M.E. Oreilly, J.A. Browning, et al., Multiple corrosion protection systems for reinforced concrete bridge components: laboratory and field tests, //2010 Concrete Bridge Conference: Achieving Safe Smart & Sustainable Bridges (2010).
[13] B. Pradhan, B. Bhattacharjee, Rebar corrosion in chloride environment, Constr. Build. Mater. 25 (5) (2011) 2565–2575.
[14] I. Martínez, C. Andrade, Polarization resistance measurements of bars embedded in concrete with different chloride concentrations: EIS and DC comparison, Mater. Corros. 62 (10) (2011) 932–942.
[15] W.H. Hartt, F. Presuelmoreno, R. Tanner, Characterization of chloride thresholds in Florida coastal concrete bridge substructures, Coasts (2009).

[16] K. Kupwadepatil, Mitigation of chloride and sulfate based corrosion in reinforced concrete via electrokinetic nanoparticle treatment, Dissertations Theses – Gradworks (2010).
[17] M. Liu, X. Cheng, X. Li, et al., Corrosion behavior of Cr modified HRB400 steel rebar in simulated concrete pore solution, Constr. Build. Mater. 93 (15) (2015) 884–890.
[18] R. Vedalakshmi, K. Rajagopal, N. Palaniswamy, Longterm corrosion performance of rebar embedded in blended cement concrete under macro cell corrosion condition, Constr. Build. Mater. 22 (3) (2008) 186–199.
[19] Y.S. Ji, M. Wu, Z. Tan, et al., Process control of reinforcement corrosion in concrete. Part 2: time-dependent dominating factors under different environmental conditions, Constr. Build. Mater. 73 (73) (2014) 214–221.
[20] S. Kakooei, H.M. Akil, A. Dolati, et al., The corrosion investigation of rebar embedded in the fibers reinforced concrete, Constr. Build. Mater. 35 (10) (2012) 564–570.
[21] H. Nahali, L. Dhouibi, H. Idrissi, Effect of phosphate based inhibitor on the threshold chloride to initiate steel corrosion in saturated hydroxide solution, Constr. Build. Mater. 50 (50) (2014) 87–94.
[22] Epoxy-coated steel for the reinforcement of concrete (GB/T25826-2010).
[23] P. Zhang, Z. Shi, About the professional standard epoxy resin coated steel bars (JG3042-1997), J. Guangxi Instit. Technol. (1997).
[24] X.K. Gao, Popularization and application of SEBF/SLF high performance epoxy coating for heavy duty anti-corrosion technology, //Conference on Corrosion and Protection of Marine Materials (2014).
[25] V. Leelalerkiet, J.W. Kyung, M. Ohtsu, et al., Analysis of half-cell potential measurement for corrosion of reinforced concrete, Constr. Build. Mater. 18 (3) (2004) 155–162.
[26] X.Q. Cheng, Y.W. Tian, X.G. Li, et al., Corrosion behavior of nickel containing weathering steel in simulated marine atmospheric environment, Mater. Corros. 8 (65) (2014) 1033–1037.
[27] Y.X. Zhao, H.Y. Ren, H. Dai, et al., Composition and expansion coefficient of rust based on X-ray diffraction and thermal analysis, Corros. Sci. 53 (2011) 1646–1658.
[28] A. Alhozaimy, R.R. Hussain, R. Al-Zaid, et al., Investigation of severe corrosion observed at intersection points of steel rebar mesh in reinforced concrete construction, Constr. Build. Mater. 37 (3) (2012) 67–81.
[29] Y.S. Ji, M. Wu, Z. Tan, et al., Process control of reinforcement corrosion in concrete. Part 2: time-dependent dominating factors under different environmental conditions, Constr. Build. Mater. 73 (73) (2014) 214–221.
[30] M.D.A. Thomas, E.C. Bentz, Life-365: computer program for predicting the service life and life-cycle costs of reinforced concrete exposed to chlorides, (2014) .
[31] K. Siamphukdee, F. Collins, R. Zou, Sensitivity analysis of corrosion rate prediction models utilized for reinforced concrete affected by chloride, J. Mater. Eng. Perform. 22 (6) (2013) 1530–1540.
[32] T. Yamaji, H. Hamada, S. Mizuma, et al., Study on the corrosion resistant property of stainless steel bars under marine environment, Jpn. Soc. Civil Eng. 66 (2) (2010) 207–220.